

Simulation and Measurement of Dielectric Charging in Electrostatically Actuated Capacitive Microwave Switches

J.R. Reid

Antenna Technology Branch
U.S. Air Force Research Laboratory, AFRL/SNHA
80 Scott Dr., Hanscom AFB, MA 01731
James.Reid@hanscom.af.mil

ABSTRACT

Simulations of the effects of dielectric charging on the operation of electrostatically actuated capacitive microwave switches have been performed. The simulations are unique in that they incorporate fixed charges into the calculation of the beam deflection. These simulations show that fixed charges in the dielectric layer cause a shift in the capacitance-voltage curve of the switch. The shift in the curve is proportional to the magnitude and depth of the charge, while the direction of the shift is determined by the polarity of the charge. Further, it is shown that sufficient charge can result in a failure of the switch to release from the dielectric layer. The simulation is confirmed by comparison with measured data.

Keywords: Microwave switches, Dielectric charging, Reliability

1 INTRODUCTION

Electrostatically actuated metal beams (Figure 1) have shown excellent potential as microwave and millimeterwave switches. Such switches have microwave performance exceeding that of other competing technologies such as PIN diodes, FETs, and HEMTs [1,2]. Further, the beams require exceptionally low power for operation and do not exhibit any intermodulation distortion.

Unfortunately, it has been widely observed that the performance of the switches can vary over time. In particular, switches can stick down when no voltage is applied, release under an applied bias, and operate with different switching voltages. It is believed that these behaviors are due to charge being injected into and trapped in the dielectric layer covering the electrode. This problem is compounded by the fact that over time and cycling, the charge in the dielectric can build up, eventually causing the switch to permanently stay closed. In fact, Goldsmith, et al., have recently reported that such charging is a major factor limiting the lifetime of their capacitive switches [3].

Simulations of clamped-clamped beams have previously focused primarily on the deflection of the beam as a function of applied voltage. Work by Osterberg, et al. [4], focused on the operation of the beam before contacting the

dielectric and does not address the problem of dielectric charging. Later work by Chan, et al. [5], used two-dimensional simulations to model not only the suspended beam, but also the beam in contact with the dielectric. However, modeling of the charging effect was limited to considering the charge as a voltage offset. In contrast, the work presented here focuses primarily on the effects of charging on deflection and operation of the beam. The simulator incorporates fixed charge into the dielectric as a function of depth, and can readily be extended to handle charge as a function of both location and depth.

Utilizing the newly coded simulator, beams with dimensions corresponding to capacitive microwave switches have been modeled under a variety of charging conditions. These simulations show that fixed charge in the dielectric results in a voltage offset that is proportional to

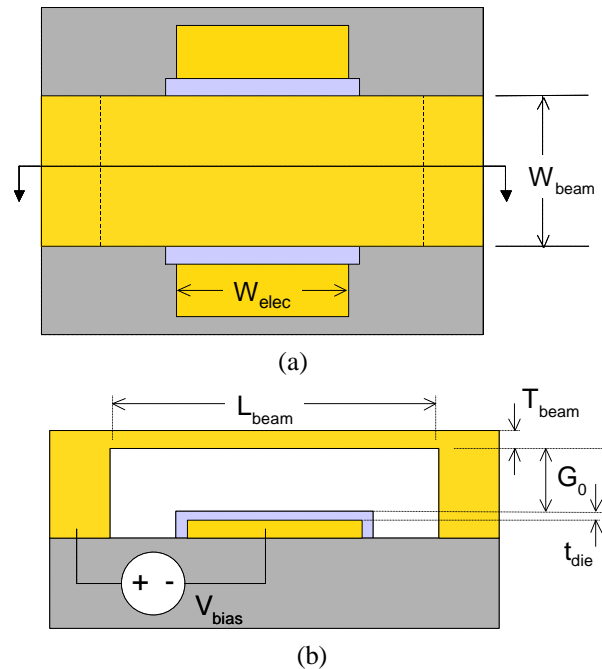


Figure 1: Schematic illustration of the electrostatically actuated clamped-clamped beam showing the primary device parameters. A top view is shown in (a), and a cross section in (b).

the magnitude, polarity, and depth of the charge in the dielectric. These results concur with the work of Chan [5] and are verified by measurements.

2 SIMULATION

2.1 Mechanical Model

The basic beam is shown in Figure 1. Across the width, the beam is considered to be uniform. Along the length, the beam is broken down into individual elements of equal length. Generally, 250 elements are used. Each element is allowed to move in only one dimension, up or down. This results in a quasi-two-dimensional model. The simulation calculates only half of the beam, mirroring the values to get a complete result. The mirroring is possible by placing the constraint that the angle of deflection at the mid-point is zero. It is assumed that both ends of the beam are rigidly clamped. The top of the dielectric is set to be the maximum deflection point, and the beam is prevented from deflecting through this point. The beam is initially considered to be at rest with a deflection of zero at all elements along the beam.

2.2 Electrostatic Model

Electrostatic calculations consist of determining the capacitance between the beam and the electrode, the charge density of the beam and the electrode, the electric field generated by the electrode and the fixed dielectric charge, and finally the force acting on the upper electrode.

The parallel-plate approximation is used to calculate the capacitance as

$$C_{seg} = \frac{\epsilon_0 \cdot W_{beam} \cdot L_{seg}}{x_{seg} + t_{norm}} \quad (1)$$

where ϵ_0 is the permittivity of air, W_{beam} is the width of the beam, L_{seg} is the length of the individual segment, x_{seg} is the distance from the top of the dielectric to the beam at each segment, and t_{norm} is the normalized thickness of the dielectric ($= t_{die}/\epsilon_r$). For typical beams, the total overlap area is on the order of $100 \mu\text{m}$ by $60 \mu\text{m}$ with a separation of $3 \mu\text{m}$ or less and thus the parallel plate approximation should introduce an error less than ten percent, which decreases as the separation is reduced. For the purposes of studying dielectric charge, small errors in the calculated values are acceptable as long as they remain consistent. As such, the corrections described by Osterberg [4] and Chan [5] have not been implemented.

For each segment, the charge density is calculated as the sum of the voltage-induced charge, $\mathbf{r}_{v,seg}$, and the image charge, $\mathbf{r}_{i,seg}$. The voltage-induced charge is the charge on the beam and electrode surfaces due to an applied bias and is calculated as

$$\mathbf{r}_{v,seg} = \frac{C_{seg} \cdot V_{bias}}{W_{beam} \cdot L_{seg}} \quad (2)$$

where V_{bias} is the potential applied to the beam. The voltage-induced charge is positive for the beam and negative for the electrode. The image charge is the charge resulting from the requirement that the system retain charge neutrality. Since a fixed charge exists in the dielectric, an image charge must form on the upper and lower electrode such that the sum of all charge is zero. This charge is calculated as

$$\mathbf{r}_{i,seg} = \sum_n R_{image}(\mathbf{a}_n) \cdot \mathbf{r}_{fixed}(\mathbf{a}_n) \quad (3)$$

where $\mathbf{r}_{fixed}(\mathbf{a}_n)$ is the fixed sheet charge density at a depth \mathbf{a}_n from the top of the dielectric, n is a user defined number of depths, and R_{image} is a ratio determining the amount of the image charge that will be on the beam or the electrode. For the beam, R_{image} is calculated as

$$R_{image}(\mathbf{a}) = R_{beam}(\mathbf{a}) = -\frac{t_{die} - \mathbf{a}}{t_{die} + x_{seg} \cdot \mathbf{e}_r} \quad (4)$$

while for the electrode R_{image} is calculated as

$$R_{image}(\mathbf{a}) = R_{elec}(\mathbf{a}) = -1 - R_{beam}(\mathbf{a}) \quad (5)$$

Given the charge densities, the field can be readily calculated by assuming that the electrode is an infinite sheet charge. This assumption is equivalent to the parallel plate approximation and thus does not introduce any new source of error. The field is then calculated for each segment as

$$\mathbf{E}_{seg} = \frac{\mathbf{r}_{elec,seg} + \sum_n \mathbf{r}_{fixed}(\mathbf{a}_n)}{2 \cdot \mathbf{e}_0} \quad (6)$$

where $\mathbf{r}_{elec,seg}$ is the charge density of the electrode at each segment. Finally, the force is simply calculated as

$$\mathbf{F}_{seg} = \mathbf{E}_{seg} \cdot \mathbf{r}_{beam,seg} \cdot W_{beam} \quad (7)$$

2.3 Deflection Calculation

Solving the deflection is done by first assuming the beam has no internal stress. The deflection is then readily solved by a numerical implementation of the method of double integration as described in reference [6]. The stress is then incorporated via iterative solution. Once a solution is found, the final deflection is compared with the initial beam state. If the change in deflection is greater than a threshold value, the entire calculation is repeated using the new beam deflection as the starting point.

Parameter	Value	Parameter	Value
W_{beam}	60 μm	G_0	1.5 μm
L_{beam}	260 μm	t_{die}	0.2 μm
T_{beam}	1 μm	σ_r	30 MPa
W_{elec}	100 μm	ϵ_r	7

Table 1: Default device simulation parameters.

3 RESULTS

All of the simulations presented here use the actuator parameters shown in Table 1 unless specifically noted. These values are typical for microwave switches. The basic output from the simulation program is a set of capacitance-voltage data pairs. Plotting this output for the switch defined in Table 1 results in the capacitance-voltage (C-V) plot shown in Figure 2. In evaluating the performance of a switch, four voltages are of primary interest. Two of these relate to the point at which the switch becomes unstable and collapses onto the dielectric. These are referred to as the positive and negative pull-in voltages, $V_{\text{pi},+}$ and $V_{\text{pi},-}$, respectively. The other two are the voltages where the switch releases from the dielectric, the positive and negative release voltages, $V_{\text{r},+}$ and $V_{\text{r},-}$, respectively. These voltages are clearly identifiable in the C-V plot (Figure 2). Adding a fixed dielectric charge and re-simulating the device results in a shift of the C-V curve as shown in Figure 3. The shape of the curve is identical to the original simulation; it has simply been offset by a small voltage. In Figure 4, it is shown that over a range of charge densities, the slope of all four voltages is the same. Thus, a single voltage offset can be used to describe the charging effect. Further, this offset is directly proportional to the magnitude of the charge and the direction of the shift is determined by the polarity of the charge. For all values in Figure 4, the charge is assumed to be a sheet charge located exactly in the middle of the dielectric. For a small amount of charging, this voltage offset is not likely to cause major problems in the operation of the switch. However, as charge builds up, it is possible to reach a state where the

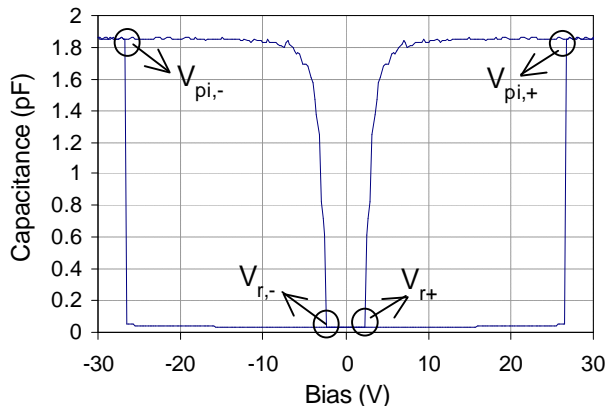


Figure 2: Simulated C-V curve for a switch with the standard parameters and no fixed dielectric charge.

positive release voltage is less than zero, or the negative release voltage is greater than zero. In these cases, a switch would stay closed and fail to operate. For the current simulations, this occurs when the magnitude of the sheet charge density exceeds $1.6 \text{ pC}/\mu\text{m}^2$. Assuming the charge is made up of either holes or electrons, this corresponds to a trap density of $10^{12}/\text{cm}^2$. This value is lower than the trap densities found in most thin dielectric films. In an operational system, the control voltage remains constant, so an increasing pull-in voltage could also result in a failure of the switch to actuate. However, this is a significantly less likely failure mode and the control voltage can be set with sufficient margin to ensure that sticking occurs before a failure to actuate. Finally, simulations of sheet charge at varying depth were performed. These simulations show that as the sheet charge moves closer to the dielectric-air interface, the magnitude of the voltage shift is increased.

Switch measurements were taken to confirm the simulation results. Measuring the switch control voltages is made difficult by rapid charging of the switch during the measurement cycle. Therefore, a microwave test setup was used instead of a capacitance meter. The switch is configured as a shunt capacitor in a co-planar waveguide as described in references [1,2]. A low power ($\approx 1\text{dBm}$), continuous wave, microwave (14.05 GHz) signal was combined with a ramp waveform. The combined signal was sent through the switch and then input into a microwave mixer for demodulation. The mixer's local oscillator was set at 14.05 GHz so that the output of the mixer is a DC value dependent upon the magnitude and phase of the switch signal, which is modulated by the motion of the beam. The resulting signal is comparable to $|S_{21}|$ of the switch. The signal and the drive voltage are recorded on an oscilloscope. The measurement takes 20-50 milliseconds, thus minimizing charging effects caused by the measurement process. Figure 5 shows data measured for a switch with design values similar to that in Table 1. Several parameters from Table 1 were adjusted to fit the measured data from the uncharged measurement. First the up- and down-state capacitances of the switch were matched by decreasing ϵ_r to 4.75, and G_0 to 1.2 μm . Note

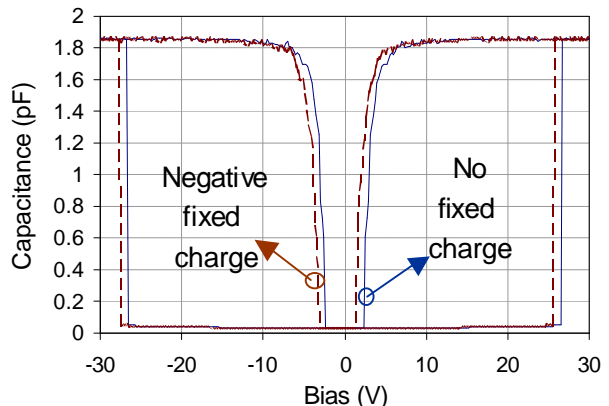


Figure 3: Simulations of the switch with and without fixed dielectric charge. The introduction of fixed charge causes the entire C-V curve to shift.

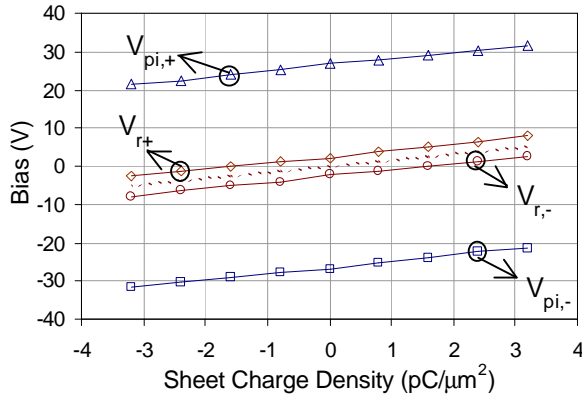


Figure 4: Simulation of the key switching voltages as a function of charge. The dotted line in the center represents the net voltage offset of the C-V curve.

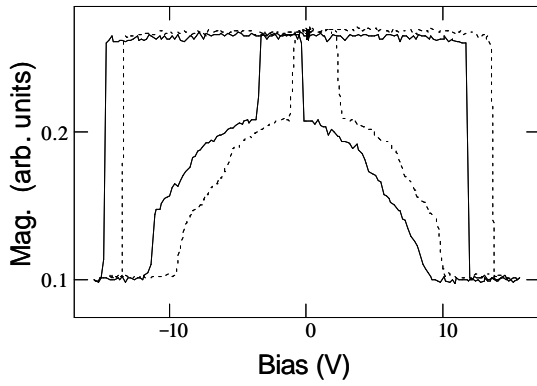


Figure 5: Measurements of a microwave switch showing a shift in the curve due to dielectric charging.

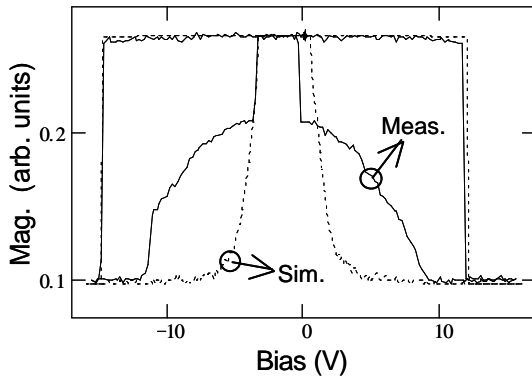


Figure 6: Comparison of simulation with measurement.

that the measured profile of the switch showed significant curvature of the beam with the switch separation around $1.0 \mu\text{m}$ at the center and increasing towards the sides of the beam. Thus, the fitted value of $1.2 \mu\text{m}$ is not unreasonable. Next, T_{beam} and σ_r were reduced to $0.94 \mu\text{m}$ and 12MPa respectively, in order to match the measured pull-in values. After these values were set, the charge in the simulation was adjusted to shift the curve. A final simulated charge density of $-0.62 \text{pC}/\mu\text{m}^2$ was used. The simulated capacitance values were then used to calculate $|S_{21}|$ for a shunt capacitor in a transmission line and compared with

the measured charge data (Figure 7) by normalizing the maximum and minimum values. Note that normalization is required because the measured values have an arbitrary scale and offset.

4 CONCLUSIONS

Quasi-two-dimensional simulations of the effects of fixed dielectric charge on the actuation of clamped-clamped beams have shown that a sheet of fixed charge in the dielectric layer results in a voltage offset in the C-V curve of the beam. This offset is directly proportional to magnitude of the fixed charge, while the direction of the shift depends on the polarity of the fixed charge. These results fit with the previous work of Chan [5], and are confirmed by measurements showing a shift in the operational voltages of a microwave switch.

These simulations also show that fixed dielectric charge changes the operational behavior of microwave MEMS switches and can cause a failure of the switch to either open or close. Further, the amount of charge required for the failure of a switch to open is consistent with trap densities commonly found in dielectric thin films. Finally, the new simulator advances previous work by directly including the charge as a function of depth and can be expanded to handle charge as a function of location.

REFERENCES

- [1] Z. Yao, S. Chen, S. Eshelman, D. Denniston, and C. Goldsmith, "Micromachined low-loss microwave switches," *Journal of Microelectromechanical Systems*, 8 (2), 129–134, 1999.
- [2] J. Rizk, G-L Tan; J. Muldavin, G. Rebeiz, "High-isolation W-band MEMS switches," *IEEE Microwave and Wireless Components Letters*, 11 (1), 10-12, 2001.
- [3] C. Goldsmith, J. Ehmke, A. Malczewski, B. Pillans, S. Eshelman, Z. Yao, J. Brank, and M. Eberly, "Lifetime characterization of capacitive RF MEMS switches," 2001 IEEE MTT-S International Microwave Symposium Digest, 1, 227-230, 2001.
- [4] P. Osterberg and S. Senturia, "M-TEST: A test chip for MEMS material property measurement using electrostatically actuated test structures," *Journal of Microelectromechanical Systems*, 6 (2), 107-118, 1997.
- [5] E. Chan, K. Garikipati and R. Dutton, "Characterization of contact electromechanics through capacitance-voltage measurements and simulations," *Journal of Microelectromechanical simulations*, 8 (2), 208-217, 1999.
- [6] M. Siegel, V. Maleev, and J. Hartman, *Mechanical design of machines*, Fourth Edition, 71-85, 1965.

ACKNOWLEDGEMENTS

The microwave test setup was put together with the help of Rick Webster (AFRL/SNHA). The microwave switches were fabricated by AFRL/SND.